

# Accepted Manuscript

Cytotoxic Activity Assessment, QSAR and Docking Study of Novel bis-Carboxamide Derivatives of 4-Pyrones Synthesized by Ugi Four-Component Reaction

Aziz Shahrissa, Somayeh Esmati, Ramin Miri, Omidreza Firuzi, Najmeh Edraki, Maryam Nejati



PII: S0223-5234(13)00372-3

DOI: [10.1016/j.ejmech.2013.05.049](https://doi.org/10.1016/j.ejmech.2013.05.049)

Reference: EJMECH 6232

To appear in: *European Journal of Medicinal Chemistry*

Received Date: 5 December 2012

Revised Date: 14 May 2013

Accepted Date: 16 May 2013

Please cite this article as: A. Shahrissa, S. Esmati, R. Miri, O. Firuzi, N. Edraki, M. Nejati, Cytotoxic Activity Assessment, QSAR and Docking Study of Novel bis-Carboxamide Derivatives of 4-Pyrones Synthesized by Ugi Four-Component Reaction, *European Journal of Medicinal Chemistry* (2013), doi: 10.1016/j.ejmech.2013.05.049.

This is a PDF file of an unedited manuscript that has been accepted for publication. As a service to our customers we are providing this early version of the manuscript. The manuscript will undergo copyediting, typesetting, and review of the resulting proof before it is published in its final form. Please note that during the production process errors may be discovered which could affect the content, and all legal disclaimers that apply to the journal pertain.

## Cytotoxic Activity Assessment, QSAR and Docking Study of Novel bis-Carboxamide Derivatives of 4-Pyrones Synthesized by Ugi Four-Component Reaction

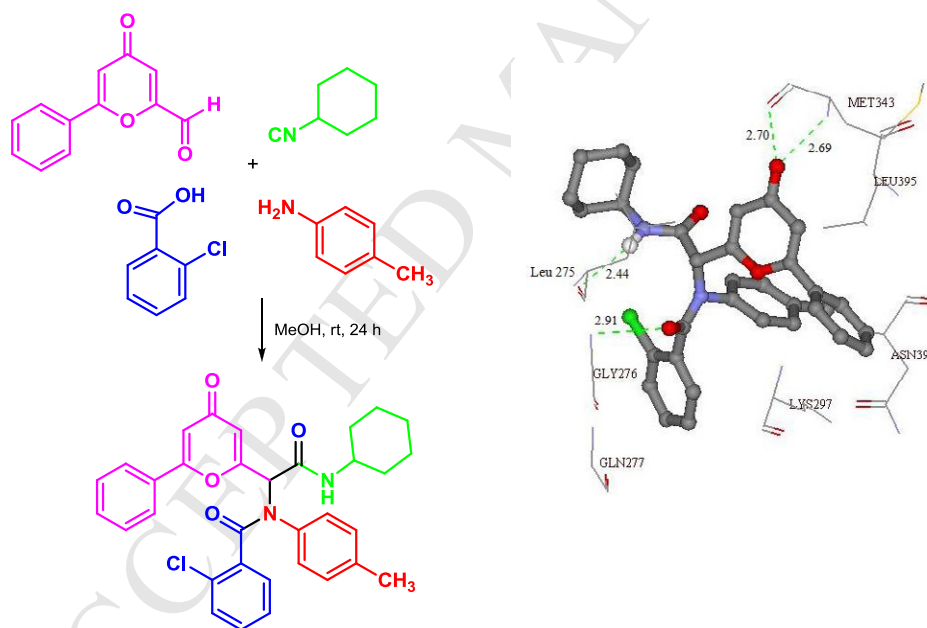
Aziz Shahrissa\*<sup>a</sup>, Somayeh Esmati<sup>a</sup>, Ramin Miri\*<sup>b</sup>, Omidreza Firuzi<sup>b</sup>, Najmeh Edraki<sup>b</sup> and Maryam Nejati<sup>b</sup>

<sup>a</sup> Department of Organic Chemistry and Biochemistry, Faculty of Chemistry, University of Tabriz, Tabriz 5166614766, Iran

<sup>b</sup> Medicinal & Natural Products Chemistry Research Centre, Shiraz University of Medical Sciences, Shiraz, Iran (phone.: +98 411 339 3118; fax: +98 411 334 0191; e-mail: [ashahrissa@yahoo.com](mailto:ashahrissa@yahoo.com) (A. Shahrissa); [mirir@sums.ac.ir](mailto:mirir@sums.ac.ir) (R. Miri))

### Graphical Abstract

A series of novel bis-carboxamide derivatives of 4-pyrones were synthesized via Ugi four component reaction and their cytotoxic activities were evaluated against three different cell lines using MTT reduction assay.



### High Lights

- New bis-amide derivatives of 4-pyrones were synthesized via Ugi 4-component reaction.
- For the first time cytotoxic activity of Ugi adducts was evaluated.

- Some of the synthesized compounds have strong cytotoxic potential in HL-60 cell line.
- The QSAR study indicated that topological properties influence cytotoxic activity.
- Docking studies of these compounds were conducted into Src tyrosine kinase.

## Abstract

Fourteen novel bis-carboxamide derivatives of 4-pyrones were designed and synthesized via Ugi four-component reactions of 4-pyronecarbaldehydes, aromatic amines, isocyanides and carboxylic acids. The cytotoxic activity of synthesized derivatives was evaluated against LS180, MCF-7 and HL-60 cell lines using MTT reduction assay. Synthesized compounds demonstrated strong cytotoxic potential in HL-60 cell line. Compound **12n** was the most potent derivative with  $IC_{50}$  values of 16.1, 9.1 and 13.8  $\mu$ M in LS180, MCF-7 and HL-60 cells, respectively. The results of MLR-QSAR study indicated that topological property of these derivatives directly influenced the cytotoxic potential in HL-60 cell line. Docking study of compounds, conducted for ATP binding site of Src tyrosine kinase, demonstrated the key H-bond interaction with Met 347 of the hinge region.

**Key words:** Ugi reaction, 4-pyrone derivatives, QSAR, Docking, Src tyrosine kinase

## 1. Introduction

4*H*-pyran-4-one (4-pyrone) derivatives constitute a promising versatile class of heterocyclic compounds, which are widely distributed in a variety of natural and synthetic biologically active compounds [1-4]. The results of different studies have indicated that amide containing 4-pyrones exhibit valuable biological activities; e.g. amidopyrones **1** are inhibitors of matrix metalloproteinases [5]. Some of amide containing 4-pyrones has been found in a variety of natural products. For example, pestalamide A **2** has been isolated from cultures of the plant pathogenic fungus *Pestalotiopsis theae* [6]. Furthermore, the anticancer and cytotoxic potential of natural and synthetic 4*H*-pyran-4-one derivatives have been well established [7-9]. Bransova and colleagues have reported the *in vitro* cytotoxic properties of different derivatives of a naturally occurring 4*H*-pyran-4-one, Kojic acid **3** (5-hydroxy-2-hydroxymethyl-4-pyrone), in leukemia

cell lines [10]. Moreover, the anticancer property of 5-benzyloxy-2-thiocyanatomethyl-4-pyrone **4** in rat pituitary carcinoma cells (GH4C1), human leukemia and murine leukemia cells has been well characterized [10,11]. In this regard, 5-benzyloxy-4-oxo-4*H*-pyran-2-carboxamides **5** (Fig. 1) have been reported as good ligands for ATP-binding site of Src tyrosine kinase [12] which plays important roles in cell growth, proliferation and invasion in many types of cancer. Therefore, Src is an attractive target for cancer chemotherapy and different types of Src inhibitors have been developed [13-15].

< Figure 1 >

On the other hand, Multicomponent reactions (MCRs) have recently become popular for preparation of pharmacologically active compounds [16]. One of the most important classes of MCRs is the isocyanide based multicomponent reaction (IMCR) [17]. Passerini developed one of the first IMCRs in 1921 [18]. This reaction was later expanded by Ugi in 1959 to afford di-amide derivatives [19] by a four-component coupling reaction of aldehyde, amine, isocyanide and carboxylic acid according to the mechanism shown in Scheme 1. Ugi reaction has widely used not only to prepare peptide-like molecules, but also have achieved profound attention for the synthesis and discovery of new lead structures and different types of biologically active scaffolds [20-28]

< Scheme 1 >

Based on the above evidences and as a part of our ongoing research on synthesis of biologically active derivatives of 4-pyrones [29-32], here we report Ugi four-component reactions for the synthesis of novel anticancer bis-carboxamide derivatives of 4*H*-pyran-4-one along with cytotoxic activity evaluation of these compounds in three different cancer cell lines including LS180, MCF-7 and HL-60 cells. Furthermore, synthesized compounds were subjected to QSAR study in order to find important structural features that influence anticancer activity of these novel derivatives. Finally, we performed a molecular docking simulation study in order to find out the binding potential of these compounds with the Src tyrosine kinase enzyme as a probable molecular target that could explain the experimental results on the cytotoxic activity.

## 2. Results and discussion

### 2.1. Chemistry

In view of interesting biological activities of pyrone motif containing carboxamide groups, we designed and synthesized new bis-amide derivatives of 4-pyrones via Ugi four component reactions. This is the first time that 4-pyrone carbaldehydes are used in Ugi reaction. As mentioned in Scheme 2 aldehyde **7** was obtained from commercially available Kojic acid **3** by benzylation of phenolic OH [33], followed by oxidation of the hydroxymethyl group with active  $\text{MnO}_2$ . Aldehyde **11** was synthesized from the corresponding ethoxycarbonyl derivative **9** according to the reported procedure [34]. The ethoxycarbonyl derivative itself was prepared through cyclization of the related 1,3,5-triketone **8** under acidic conditions, which is an important method for the synthesis of a variety of 4-pyrone derivatives [35-37].

< Scheme 2 >

As shown in the Scheme 3, novel Ugi products **12a-n** were synthesized by the reaction of 4-pyrone carbaldehydes, isocyanides, carboxylic acids and amines in the absence of any catalyst in methanol. The reaction mixtures were stirred at room temperature for 24 hours and the final products were obtained with good yields. The results are summarized in Table 1. This method is simple and convenient and would be applicable for the synthesis of different types of 4-pyrone bis-amides, since operates at room temperature under catalyst-free condition.

< Scheme 3 >

< Table 1 >

The structures of final products were confirmed by  $^1\text{H}$  NMR,  $^{13}\text{C}$  NMR, FT-IR and elemental analysis.

## 2.2. Cytotoxic activity

The *in vitro* anti-cancer activity of target compounds **12a-n** was determined against LS 180 (intestinal human colon adenocarcinoma cells), MCF-7 (breast cancer human cell lines) and HL60 (human promyelocytic leukemia cell line) cells using MTT 3-(4,5-dimethylthiazol-2-yl)-2,5-diphenyltetrazolium bromide method [38]. Briefly, cell viability was assessed by MTT colorimetric assay in which the viable cell number is directly proportional to the production of purple formazan. This color product can be measured spectrophotometrically at 570 nm by an ELISA plate reader. The percent inhibition of viability for each concentration of compound was

calculated compared to the control wells and  $IC_{50}$  values (concentration of the compound that induces 50% inhibition of cell viability) were calculated by linear regression and expressed in Mean  $\pm$  SD. The results are represented in Table 2.

< Table 2 >

The results of cytotoxic data indicate that most of synthesized compounds showed moderate to strong cytotoxic potential especially in HL-60 and MCF-7 cell lines. Although all synthesized bis-carboxamide derivatives of 4-pyrones possess lower cytotoxic potential than doxorubicin in all three cell lines, some of them showed superior potency to cisplatin especially in MCF-7 and HL-60 cell lines (compounds **12e** in MCF-7 and **12n** in HL-60 cells).

According to the  $R_1$ ,  $R_2$ ,  $R_3$  and  $R_4$  substituents shown in Fig. 2 and based on the cytotoxic data in Table 2, the following structure-activity relationship may be developed:

< Figure 2 >

The compounds could be classified into two groups according to the  $R_1$  substituent: benzyloxy-4-pyrones (**12a-i**) and phenyl-4-pyrone derivatives (**12j-n**). The benzyloxy derivatives of 4-pyrones demonstrated more cytotoxic potential than phenyl-4-pyrones in some cases. For instance, the benzyloxy derivative **12c** is more potent than its phenyl-4-pyrone counterpart **12k** in all three cell lines;  $IC_{50}$  values for **12c** against HL-60, LS180 and MCF-7 were 12.1, 63.0 and 56.3  $\mu$ M, respectively, while **12k** was inactive in two first lines and its  $IC_{50}$  value against HL-60 cells was 22.2  $\mu$ M.

$R_2$  moiety in the synthesized compounds could be cyclohexyl or *t*-butyl. There was no significant difference in the cytotoxic potency of cyclohexyl and *t*-butyl bearing derivatives. However, by considering the substitution pattern on  $R_3$  group, some differences were observed between cyclohexyl and *t*-butyl derivatives: The introduction of 2-chlorophenyl in the  $R_3$  moiety enhanced cytotoxic potential of *t*-butyl bearing derivatives, while it reduced the potency of cyclohexyl bearing derivatives. For instance, it is noteworthy to compare activity of compounds **12c** and **12e** which possessing cyclohexyl at  $R_2$  ( $R_1$  and  $R_4$  groups are also the same in **12c** and **12e**). Compound **12e** with phenyl group as  $R_3$ , showed significant cytotoxic potential against all three cell lines ( $IC_{50}$  values in HL-60, LS180 and MCF-7 cell lines were 11.3, 20.2 and 11.2  $\mu$ M, respectively), while compound **12c** with 2-chlorophenyl as  $R_3$  showed lower potency especially against LS180 and MCF-7 cell line ( $IC_{50}$ = 63.0 and 56.3  $\mu$ M respectively). This observation may

be described as a result of geometrical hindrance imposed in cyclohexyl derivatives by introduction of chlorine atom into R<sub>3</sub>-phenyl moiety, which can hinder the ligand-receptor access. However, this substitution pattern in *t*-butyl containing derivatives caused the inverse outcome, as exemplified in the comparison of the activity of compounds **12l** and **12n**. Compound **12l** containing phenyl moiety as R<sub>3</sub> showed lower activity than its 2-chlorophenyl analog **12n** in all three cell lines. Thus compound **12n** is one of the promising synthesized derivatives in all three cell lines (IC<sub>50</sub> values in HL-60, LS180 and MCF-7 cell lines were 13.8, 16.1 and 9.1, respectively).

On the other hand, the results indicated that the introduction of different substituents such as methyl, *n*-butyl, methoxy and chlorine in *para* position of phenyl in R<sub>4</sub> moiety resulted in enhanced cytotoxic potential of compounds in both series of pyrone derivatives (benzyloxy and phenylpyrones) especially in HL-60 cell line; e.g. the corresponding IC<sub>50</sub> value for compound **12a** containing phenyl group at R<sub>4</sub> (Y=H) in HL-60 cell lines is 66.2 μM. Introduction of methyl group in *para* position of phenyl ring (Z=methyl, **12c**) considerably enhances the cytotoxic potency of this compound in these cells (IC<sub>50</sub>=12.1 μM).

### 2.3. QSAR study

QSAR analysis of synthetic compounds (**12a-n**) was carried out by MLR analysis. The correlation coefficient (R<sup>2</sup>), standard error of regression (SE), correlation coefficient for cross-validation significance (Q<sup>2</sup>) and root mean square error (RMS) were employed to judge the validity of regression equation. As collinearity degrades the performances of the MLR based QSAR equation, correlation analysis was performed to detect the collinear descriptors (Mager, 1983). Therefore, the correlation of descriptors with each other and with activity data was evaluated and among the collinear descriptors one of them that represented the highest correlation with activity was retained and the rest were omitted.

Due to limited available cytotoxic data in LS180 and MCF-7 cell lines (8 and 10 respectively), no valid QSAR model is obtained for quantitative structure-activity elucidation of bis-amide derivatives of pyrone in these two cell lines.

When we used pIC<sub>50</sub> of bis-carboxamide derivatives of pyrone against HL-60 cell line as dependent variable the three parametric equation E1 with good statistical quality was obtained

from the pool of calculated descriptors ( $R^2=0.93$ , S.E.= 0.09 and  $Q^2=0.83$ ) (Table 3). Selected variables indicated that topological property (PJI2: 2D petitjean shape index) of bis-amide 4-pyrones directly affect the cytotoxic potential of compounds against HL-60 cell line. Whereas, GETAWAY parameters including HGM (geometric mean on the leverage magnitude) and ISH (standardized information content on the leverage equality) demonstrated negative relation with cytotoxic potency of compounds in these cells.

< Table 3 >

The data of selected descriptors used in this study together with the experimental and corresponding predicted value of activity of compounds such as pIC<sub>50</sub> (-Log IC<sub>50</sub>) are listed in Table 4. The respective predicted values of activity, refined from the calibration and cross-validation, by using equation 1 is plotted against the experimental values. As it could be seen, there is a close agreement between the experimental and predicted activities obtained by QSAR model in HL-60 cell line (Fig. 3.)

< Table 4 >

< Figure 3 >

#### 2.4. Docking study

Based on the crystal structure of active Src tyrosine kinase inhibitor 1-{4-[4-amino-5-(3-methoxyphenyl)-7H-pyrrolo[2,3-D]pyrimidin-7-yl]benzyl}piperidin-4-ol (S03) (PDB ID: 1YOL) [39] we docked the bis-carboxamide derivatives of 4-pyrone into ATP site of this enzyme using Autodock 4.2 software by flexible ligand/rigid macromolecule protocol. Docking optimization and validation was performed according to the cited method based on the RMSD (root mean square deviation) of the best-docked conformation of cognate ligand from experimental one (internal validation) [40]. Docking performance examined by re-docking the co-crystallized conformation of a native ligand (S03) to Src tyrosine kinase ATP site. The best-docked and actual conformation of inhibitor superimposed quite well with an RMSD of 1.463 Å (The RMSD value of below 2 Å is considered as an index of successful prediction [41]). The results of internal validation along with important binding interactions are reported in Table 5. This inhibitor produces a key hydrogen bonding interaction with Met 343 of hinge region of the active

site, which is important for directing the ligand for other hydrogen bonding interaction with Src gate keeper residue Thr340 and also with Glu342. Moreover the 3-methoxyphenyl moiety of the ligand is mainly oriented towards the hydrophobic backpocket of the enzyme and produces important hydrophobic interactions with this pocket.

< Table 5 >

As described by Farard and co-workers [12], the 4-pyrone moiety could be served as a hydrogen-bond acceptor moiety for interaction with the hinge region of Src tyrosine kinase. Therefore, we performed a docking study on the synthesized bis-amide derivatives of 4-pyrones into the active site of Src tyrosine kinase to further evaluate the binding affinity of these compounds into ATP site of this enzyme. Docking results including free binding energies ( $\Delta G_b$ ), inhibition constants ( $K_i$ ) and hydrogen bonds are demonstrated in Table 6. Top ranked binding energies (kcal/mol) in AutoDock dlG output file were considered as response in each run.

< Table 6 >

Some of these derivatives (**12a**, **12g**, **12j**, **12k** and **12n**) demonstrated key hydrogen-bonding interaction with Met 343 of hinge region. The carbonyl group of 4-pyrone moiety is mainly involved in this interaction in cyclohexyl containing derivatives (**12a**, **12j** and **12k**), while in *t*-butyl containing derivatives the different orientation was observed, since other part of molecule participated in this key H-bond interaction. The binding interaction of the most potent cytotoxic derivative **12n** containing *t*-butyl moiety as  $R_2$  group is depicted in Fig. 4A. The  $R_4$  substituent is oriented towards the hinge region; since the methoxy group substituted on the *para* position of phenyl ring produced H-bond interaction with Met343. These parts of ligand ( $R_4$ ) along with 2-chlorophenyl group ( $R_3$ ) are involved in hydrophobic interaction with the backpocket of active site (composed of Lys 297 and Leu275) as observed in S03 binding pose. The other important interactions are depicted in Fig. 4A. The attached phenyl moiety on the  $C_2$  position of 4-pyrone ring oriented toward Thr340. Accordingly, substitution of suitable groups in this part could provide the other important H-bonding with this residue. On the other hand, as it is depicted in Fig. 4B, the  $R_4$  (*p*-methylphenyl) and  $R_3$  (2-chlorophenyl) substitute of cyclohexyl containing derivative **12k** also oriented toward the backpocket and involved in important hydrophobic

interaction with this part of active site. As mentioned previously, the pyrone moiety of **12k** is directed toward hinge part to provide the key H-bond interaction with this part.

Overall, the results of the docking study indicate that the binding orientation of bis-carboxamide derivatives towards the hinge region is mainly dependent on the substituted moiety on the R<sub>4</sub> position of this scaffold. Regarding this substitution, cyclohexyl derivatives demonstrated different binding orientation than *t*-butyl ones. This effect could be interpreted with the results of QSAR study that topological descriptors influence the cytotoxic activity of bis-carboxamide derivatives of 4-pyrones. It could be concluded that the R<sub>4</sub> substitute might topologically affects ligand-protein interaction. Furthermore, new H-bond interactions with Leu 275, Ser 347, Asp 350, Gln 377 and Ala 390 residues were detected for these new 4-pyrone derivatives. The results indicate that attachment of suitable groups with H-bond interacting potential into C-2 position of the 4-pyrone ring would result in the other important H-bond interaction with Thr340 residue of active site and should be noticed in development of potent Src tyrosine kinase inhibitors of this type.

< Figure 4 >

### 3. Conclusions

In conclusion, we have described an efficient Ugi four-component reaction for the synthesis of novel bis-amide derivatives of 4-pyrones under mild and neutral reaction conditions. This method for synthesis of bis-amide derivatives has the advantages of simple operation in one-pot and room temperature reaction conditions, simple experimental work up procedures and good yields. These derivatives demonstrated considerable cytotoxic potential especially in HL-60 cell line, which was mainly dependent on the topological properties of the molecule as revealed by QSAR study. Inhibition of Src tyrosine kinase enzyme might be considered as one of the probable cytotoxic mechanisms of these compounds. However; different cytotoxic profiles of these compounds indicate that other molecular targets might be involved for anticancer activity of these derivatives.

### 4. Experimental protocols

#### 4.1. Chemistry

Melting points were determined with a MEL-TEMP model 1202D and are uncorrected. FT-IR spectra were recorded on a Bruker Tensor 27 spectrometer as KBr disks. The  $^1\text{H}$  NMR spectra were recorded with a Bruker Spectrospin Avance 400 spectrometer with  $\text{CDCl}_3$  as solvent and TMS as internal standard.  $^{13}\text{C}$  NMR spectra were determined on the same instrument at 400 MHz. All chemical shifts were reported as  $\delta$  (ppm) and coupling constants ( $J$ ) are given in Hz. Elementray analyses (C, H, N) were performed on a Vario EL III analyzer. Thin-layer chromatography was done with prepared glass-backed plates ( $20 \times 20 \text{ cm}^2$ ,  $500 \mu$ ) using silica gel (Merk Kieselgel 60 HF<sub>254</sub>, Art. 7739). The chemical reagents used in synthesis were purchased from Merck and Sigma-Aldrich.

##### 4.1.1. Procedure for the synthesis of 4-pyrone carbaldehydes **7** and **11**

Alcohol derivatives (**6**) or (**10**) (2.4 mmol) was dissolved in dichloromethane ( $20 \text{ cm}^3$ ) and activated manganese (IV) oxide (21 mmol) was added. The reaction mixture was stirred efficiently for 3 days at room temperature then the black suspension was filtered through a pad of silica, which was washed with warm ethyl acetate ( $50 \text{ cm}^3$ ). The resulting solution was evaporated under reduced pressure and the crude product was purified by recrystallization from chloroform/ethanol to give the pure aldehyde.

##### 4.1.1.1. 5-Benzyloxy-4-Oxo-4H-pyran-2-carbaldehyde (**7**)

Pale yellow solid; Yield: 65%; mp: 118-120°C; FT-IR (KBr):  $\nu$  3087, 2923, 2860 (aldehyde CH), 1713 (aldehyde C=O), 1647 (pyrone C=O), 1615, 1211, 1139  $\text{cm}^{-1}$ ;  $^1\text{H}$  NMR (400 MHz,  $\text{CDCl}_3$ ):  $\delta$  5.16 (s, 2H,  $\text{OCH}_2\text{Ph}$ ), 7.02 (s, 1H, H-3 pyrone), 7.36–7.43 (m, 5H, Ph-H), 7.69 (s, 1H, H-6 pyrone), 9.67 (s, 1H, CHO) ppm.

##### 4.1.1.2. 4-Oxo-6-phenyl-4H-pyran-2-carbaldehyde (**11**)

Pale yellow solid; Yield: 62%; mp: 115-116°C; FT-IR (KBr):  $\nu$  3046, 2858 (aldehyde C–H), 2733 (aldehyde C–H), 1714 (aldehyde C=O), 1647 (pyrone C=O)  $\text{cm}^{-1}$ ;  $^1\text{H}$  NMR (400 MHz,  $\text{CDCl}_3$ ):  $\delta$  6.89 (d, 1H,  $J = 2 \text{ Hz}$ , pyrone-H), 6.93 (d, 1H,  $J = 2 \text{ Hz}$ , pyrone-H), 7.49-7.58 (m, 3H, Ph-H), 7.84-7.87 (m, 2H, Ph-H), 9.76 (s, 1H, –CHO) ppm;  $^{13}\text{C}$  NMR (100 MHz,  $\text{CDCl}_3$ ):  $\delta$  112.1, 120.6, 125.2, 128.2, 129.2, 131.2, 155.6, 162.8, 178.4, 183.3 ppm.

#### 4.1.2. General procedure for the synthesis of Ugi products **12a-n**

A mixture of pyrone carbaldehydes **7** or **11** (0.5 mmol) and suitable amine ( $R_4-NH_2$ ) (0.5 mmol) in MeOH (2 ml) was stirred for 30 min at room temperature and then carboxylic acid ( $R_3-COOH$ ) (0.5 mmol) and isocyanide ( $R_2-NC$ ) (0.6 mmol) was added and reaction mixture was stirred at room temperature for 24h (The progress of reaction was monitored by TLC). After completion of reaction, the residue was purified by preparative thin layer chromatography PTLC (silica gel, acetone- *n*-hexane, 1:3) to give corresponding products **12a-n**.

##### 4.1.2.1. *N*-[(5-(Benzyloxy)-4-oxo-4H-pyran-2-yl)-(cyclohexylcarbamoyl)-methyl]-2-chloro-*N*-phenylbenzamide (**12a**)

Pale yellow solid; Yield: 84%; mp: 65-67°C; FT-IR (KBr):  $\nu$  3294 (N-H), 3068 (aromatic C-H), 2929 (aliphatic C-H), 2854 (aliphatic C-H), 1695 (amide C=O), 1647 (pyrone C=O)  $cm^{-1}$ ;  $^1H$  NMR (400 MHz,  $CDCl_3$ ):  $\delta$  1.09–1.94 (m, 10H, 5CH<sub>2</sub> of cyclohexyl), 3.83 (m, 1H, CH–N of cyclohexyl), 4.96 (d, 1H,  $J$ = 12 Hz, benzylic-H), 5.01 (d, 1H,  $J$ = 12 Hz, benzylic-H), 5.97 (s, 1H, C-H), 6.62 (s, 1H, pyrone-H), 6.93 (bd, 1H,  $J$ = 8 Hz, N-H), 7.03-7.08 (m, 9H, Ar-H), 7.27-7.35 (m, 5H, Ar-H), 7.43 (s, 1H, pyrone-H) ppm;  $^{13}C$  NMR (100 MHz,  $CDCl_3$ ):  $\delta$  23.6, 23.7, 24.3, 31.4, 31.5, 48.1, 62.8, 70.6, 116.1, 125.2, 126.7, 127.3, 127.5, 127.6, 127.6, 127.7, 127.8, 128.3, 129.2, 129.2, 133.9, 134.3, 137.9, 140.3, 145.9, 159.0, 163.3, 167.9, 173.1 ppm; Anal. Calcd. For  $C_{33}H_{31}ClN_2O_5$ : C, 69.41; H, 5.47; N, 4.91; Found: C, 69.23; H, 5.38; N, 4.86%

##### 4.1.2.2. *N*-[(5-(Benzyloxy)-4-oxo-4H-pyran-2-yl)-(tert-butylcarbamoyl)-methyl]-*N*-phenylbenzamide (**12b**)

Pale yellow solid; Yield: 78%; mp: 62-63°C; FT-IR (KBr):  $\nu$  3308 (N-H), 3069 (aromatic C-H), 2963 (aliphatic C-H), 2924 (aliphatic C-H), 2858 (aliphatic C-H), 1692 (amide C=O), 1644 (pyrone C=O)  $cm^{-1}$ ;  $^1H$  NMR (400 MHz,  $CDCl_3$ ):  $\delta$  1.35 (s, 9H, 3 CH<sub>3</sub>), 4.97 (d, 1H,  $J$ = 12 Hz, benzylic-H), 5.02 (d, 1H,  $J$ = 12 Hz, benzylic-H), 5.87 (s, 1H, C-H), 6.53 (bs, 1H, N-H), 6.65 (s, 1H, pyrone-H), 7.12-7.34 (m, 15H, Ar-H), 7.44 (s, 1H, pyrone-H) ppm;  $^{13}C$  NMR (100 MHz,  $CDCl_3$ ):  $\delta$  27.5, 51.1, 64.6, 70.9, 115.7, 126.7, 126.8, 126.9, 127.3, 127.4, 127.6, 127.7, 127.8, 128.1, 129.3, 133.5, 134.5, 139.9, 140.6, 146.0, 159.7, 163.6, 170.2, 173.2 ppm; Anal. Calcd. For  $C_{31}H_{30}N_2O_5$ : C, 72.92; H, 5.92; N, 5.49; Found: 72.75; H, 5.95; N, 5.41%

4.1.2.3. *N*-[(5-(Benzyloxy)-4-oxo-4*H*-pyran-2-yl)-(cyclohexylcarbamoyl)-methyl]-2-chloro-*N*-*p*-tolylbenzamide (**12c**)

Pale yellow solid; Yield: 88%; mp: 67-68°C; FT-IR (KBr):  $\nu$  3295 (N-H), 3069 (aromatic C-H), 2930 (aliphatic C-H), 2855 (aliphatic C-H), 1682 (amide C=O), 1649 (pyrone C=O)  $\text{cm}^{-1}$ ;  $^1\text{H}$  NMR (400 MHz,  $\text{CDCl}_3$ ):  $\delta$  1.11-1.92 (m, 10H, 5 $\text{CH}_2$  of cyclohexyl), 2.14 (s, 3H,  $\text{CH}_3$ ), 3.80 (m, 1H, CH-N of cyclohexyl), 4.96 (d, 1H,  $J$ = 12 Hz, benzylic-H), 5.00 (d, 1H,  $J$ = 12 Hz, benzylic-H), 5.99 (s, 1H, C-H), 6.58 (s, 1H, pyrone-H), 6.84 (d, 2H,  $J$ = 8 Hz, Ar-H), 7.04-7.18 (m, 7H, Ar-H, N-H), 7.31-7.35 (m, 5H, Ar-H), 7.46 (s, 1H, pyrone-H) ppm;  $^{13}\text{C}$  NMR (100 MHz,  $\text{CDCl}_3$ ):  $\delta$  19.9, 23.6, 23.7, 24.3, 31.5, 31.6, 48.1, 62.8, 70.7, 116.2, 125.3, 126.7, 126.9, 127.3, 127.4, 127.5, 127.6, 128.3, 128.5, 129.1, 134.1, 134.4, 135.3, 137.5, 140.3, 145.9, 158.9, 163.3, 168.1, 173.0 ppm; Anal. Calcd. For  $\text{C}_{34}\text{H}_{33}\text{ClN}_2\text{O}_5$ : C, 69.80; H, 5.68; N, 4.79; Found: C, 69.62; H, 5.71; N, 4.70%

4.1.2.4. *N*-[(5-(Benzyloxy)-4-oxo-4*H*-pyran-2-yl)-(tert-butylcarbamoyl)-methyl]-2-chloro-*N*-*p*-tolylbenzamide (**12d**)

Pale yellow solid; Yield: 85%; mp: 60-62°C; FT-IR (KBr):  $\nu$  3303 (N-H), 3075 (aromatic C-H), 2966 (aliphatic C-H), 2924 (aliphatic C-H), 2865 (aliphatic C-H), 1687 (amide C=O), 1646 (pyrone C=O)  $\text{cm}^{-1}$ ;  $^1\text{H}$  NMR (400 MHz,  $\text{CDCl}_3$ ):  $\delta$  1.39 (s, 9H, 3  $\text{CH}_3$ ), 2.16 (s, 3H,  $\text{CH}_3$ ), 4.97 (d, 1H,  $J$ = 12 Hz, benzylic-H), 5.02 (d, 1H,  $J$ = 12 Hz, benzylic-H), 5.82 (s, 1H, C-H), 6.61 (s, 1H, pyrone-H), 6.73 (bs, 1H, N-H), 6.86 (d, 2H,  $J$ = 8Hz, Ar-H), 7.02-7.19 (m, 6H, Ar-H), 7.30-7.38 (m, 5H, Ar-H), 7.46 (s, 1H, pyrone-H) ppm;  $^{13}\text{C}$  NMR (100 MHz,  $\text{CDCl}_3$ ):  $\delta$  19.9, 27.4, 51.0, 63.5, 70.7, 116.0, 125.2, 126.7, 127.2, 127.3, 127.5, 128.3, 128.4, 129.0, 129.1, 134.1, 134.4, 135.4, 137.4, 140.3, 145.9, 159.2, 163.3, 168.0, 173.0 ppm; Anal. Calcd. For  $\text{C}_{32}\text{H}_{31}\text{ClN}_2\text{O}_5$ : C, 68.75; H, 5.59; N, 5.01; Found: C, 68.67; H, 5.61; N, 4.97%

4.1.2.5. *N*-[(5-(Benzyloxy)-4-oxo-4*H*-pyran-2-yl)-(cyclohexylcarbamoyl)-methyl]-*N*-*p*-tolylbenzamide (**12e**)

Pale yellow solid; Yield: 78%; mp: 95-97°C; FT-IR (KBr):  $\nu$  3240 (N-H), 3051 (aromatic C-H), 2989 (aliphatic C-H), 2927 (aliphatic C-H), 2854 (aliphatic C-H), 1677 (amide C=O), 1643

(pyrone C=O)  $\text{cm}^{-1}$ ;  $^1\text{H}$  NMR (400 MHz,  $\text{CDCl}_3$ ):  $\delta$  1.11-1.90 (m, 10H,  $5\text{CH}_2$  of cyclohexyl), 2.21 (s, 3H,  $\text{CH}_3$ ), 3.80 (m, 1H, CH-N of cyclohexyl), 4.97 (d, 1H,  $J=12$  Hz, benzylic-H), 5.02 (d, 1H,  $J=12$  Hz, benzylic-H), 5.92 (s, 1H, C-H), 6.61 (s, 1H, pyrone-H), 6.77 (bd, 1H,  $J=8$  Hz, N-H), 6.91 (d, 2H,  $J=8$  Hz, Ar-H), 6.96 (d, 2H,  $J=8$  Hz, Ar-H), 7.14-7.17 (m, 2H, Ar-H), 7.23-7.35 (m, 8H, Ar-H), 7.45 (s, 1H, pyrone-H) ppm;  $^{13}\text{C}$  NMR (100 MHz,  $\text{CDCl}_3$ ):  $\delta$  19.9, 23.6, 24.3, 31.5, 31.6, 47.9, 64.0, 70.7, 115.7, 126.7, 126.8, 127.4, 127.5, 127.6, 128.7, 129.2, 131.6, 133.6, 134.5, 136.9, 137.2, 140.3, 145.9, 159.5, 163.7, 170.4, 173.1 ppm; Anal. Calcd. For  $\text{C}_{34}\text{H}_{34}\text{N}_2\text{O}_5$ : C, 74.16; H, 6.22; N, 5.09; Found: C, 74.01; H, 6.25; N, 5.01%

4.1.2.6. *N-[(5-(Benzyloxy)-4-oxo-4H-pyran-2-yl)-(tert-butylcarbamoyle)-methyl]-N-(4-butylphenyl)-2-chlorobenzamide (12f)*

Pale yellow solid; Yield: 82%; mp: 70-72°C; FT-IR (KBr):  $\nu$  3296 (N-H), 3081 (aromatic C-H), 2960 (aliphatic C-H), 2927 (aliphatic C-H), 2861 (aliphatic C-H), 1679 (amide C=O), 1647 (pyrone C=O)  $\text{cm}^{-1}$ ;  $^1\text{H}$  NMR (400 MHz,  $\text{CDCl}_3$ ):  $\delta$  0.84 (t, 3H,  $J=8$  Hz,  $\text{CH}_3$ ), 1.14-1.23 (m, 2H,  $\text{CH}_2$ ), 1.39-1.46 (m, 11H,  $3\times\text{CH}_3$ ,  $\text{CH}_2$ ), 2.43 (t, 2H,  $J=8$  Hz,  $\text{CH}_2$ ), 4.97 (d, 1H,  $J=12$  Hz, benzylic-H), 5.03 (d, 1H,  $J=12$  Hz, benzylic-H), 5.78 (s, 1H, C-H), 6.62 (s, 1H, pyrone-H), 6.75 (bs, 1H, N-H), 6.87 (d, 2H,  $J=8$  Hz, Ar-H), 6.99-7.19 (m, 6H, Ar-H), 7.27-7.36 (m, 5H, Ar-H), 7.46 (s, 1H, pyrone-H) ppm;  $^{13}\text{C}$  NMR (100 MHz,  $\text{CDCl}_3$ ):  $\delta$  12.8, 20.9, 27.4, 31.9, 33.9, 51.1, 63.9, 70.7, 115.9, 125.2, 126.7, 127.2, 127.3, 127.5, 127.6, 127.8, 128.3, 129.1, 129.2, 134.0, 134.5, 135.7, 140.3, 142.4, 146.0, 159.2, 163.4, 168.1, 173.1 ppm; Anal. Calcd. For  $\text{C}_{35}\text{H}_{37}\text{ClN}_2\text{O}_5$ : C, 69.93; H, 6.20; N, 4.66; Found: C, 69.74; H, 6.23; N, 4.59%

4.1.2.7. *N-[(5-(Benzyloxy)-4-oxo-4H-pyran-2-yl)-(tert-butylcarbamoyle)-methyl]-2-chloro-N-(4-methoxyphenyl) benzamide (12g)*

Pale yellow solid; Yield: 72%; mp: 90-92°C; FT-IR (KBr):  $\nu$  3304 (N-H), 3073 (aromatic C-H), 2966 (aliphatic C-H), 2927 (aliphatic C-H), 1682 (amide C=O), 1647 (pyrone C=O)  $\text{cm}^{-1}$ ;  $^1\text{H}$  NMR (400 MHz,  $\text{CDCl}_3$ ):  $\delta$  1.41 (s, 9H, 3  $\text{CH}_3$ ), 3.67 (s, 3H,  $\text{CH}_3$ ), 4.98 (d, 1H,  $J=12$  Hz, benzylic-H), 5.04 (d, 1H,  $J=12$  Hz, benzylic-H), 5.82 (s, 1H, C-H), 6.56 (bs, 1H, N-H), 6.58 (s, 1H, pyrone-H), 6.60 (d, 2H,  $J=4$  Hz, Ar-H), 7.07-7.20 (m, 6H, Ar-H), 7.31-7.34 (m, 5H, Ar-H), 7.45 (s, 1H, pyrone-H) ppm;  $^{13}\text{C}$  NMR (100 MHz,  $\text{CDCl}_3$ ):  $\delta$  27.5, 51.1, 54.2, 63.3, 70.8, 112.9, 116.3, 125.3, 126.7, 127.4, 127.5, 127.6, 128.3, 128.8, 129.1, 130.5, 134.2, 134.5, 140.5, 145.9,

158.1, 159.0, 163.4, 168.3, 173.0 ppm; Anal. Calcd. For  $C_{32}H_{31}ClN_2O_6$ : C, 66.84; H, 5.43; N, 4.87; Found: C, 66.60; H, 5.39; N, 4.71%

4.1.2.8. *N*-[(5-(Benzyloxy)-4-oxo-4*H*-pyran-2-yl)-(cyclohexylcarbamoyl)-methyl]-2-chloro-*N*-(4-chlorophenyl)benzamide (**12h**)

Pale yellow solid; Yield: 74%; mp: 60-62°C; FT-IR (KBr):  $\nu$  3297 (N-H), 3072 (aromatic C-H), 2929 (aliphatic C-H), 2855 (aliphatic C-H), 1682 (amide C=O), 1649 (pyrone C=O)  $cm^{-1}$ ;  $^1H$  NMR (400 MHz,  $CDCl_3$ ):  $\delta$  1.12–1.91 (m, 10H, 5 $CH_2$  of cyclohexyl), 3.80 (m, 1H, CH–N of cyclohexyl), 4.97 (d, 1H,  $J$ = 12 Hz, benzylic-H), 5.02 (d, 1H,  $J$ = 12 Hz, benzylic-H), 6.01 (s, 1H, C-H), 6.58 (s, 1H, pyrone-H), 6.75 (bd, 1H,  $J$ = 8 Hz, N-H), 7.00-7.21 (m, 8H, Ar-H), 7.32-7.39 (m, 5H, Ar-H), 7.41 (s, 1H, pyrone-H) ppm;  $^{13}C$  NMR (100 MHz,  $CDCl_3$ ):  $\delta$  23.6, 23.7, 24.3, 31.4, 31.5, 48.3, 62.1, 70.7, 116.5, 125.4, 126.7, 127.4, 127.5, 127.6, 127.7, 127.9, 128.4, 129.1, 129.3, 129.4, 133.4, 133.8, 134.2, 136.2, 140.5, 145.9, 158.7, 163.1, 167.7, 172.9 ppm; Anal. Calcd. For  $C_{33}H_{30}Cl_2N_2O_5$ : C, 65.46; H, 4.99; N, 4.63; Found: C, 65.39; H, 5.02; N, 4.58%

4.1.2.9. *N*-[(5-(Benzyloxy)-4-oxo-4*H*-pyran-2-yl)-(cyclohexylcarbamoyl)-methyl]-*N*-(4-chlorophenyl)benzamide (**12i**)

Pale yellow solid; Yield: 71%; mp: 64-66°C; FT-IR (KBr):  $\nu$  3301 (N-H), 3067 (aromatic C-H), 2928 (aliphatic C-H), 2854 (aliphatic C-H), 1677 (amide C=O), 1645 (pyrone C=O)  $cm^{-1}$ ;  $^1H$  NMR (400 MHz,  $CDCl_3$ ):  $\delta$  1.12–1.90 (m, 10H, 5 $CH_2$  of cyclohexyl), 3.78 (m, 1H, CH–N of cyclohexyl), 4.97 (d, 1H,  $J$ = 12 Hz, benzylic-H), 5.02 (d, 1H,  $J$ = 12 Hz, benzylic-H), 6.02 (s, 1H, C-H), 6.58 (d, 1H,  $J$ = 2Hz, pyrone-H), 6.66 (bd, 1H,  $J$ = 8 Hz, N-H), 6.99-7.37 (m, 14H, Ar-H), 7.39 (s, 1H, pyrone-H) ppm;  $^{13}C$  NMR (100 MHz,  $CDCl_3$ ):  $\delta$  23.6, 23.7, 24.3, 31.5, 31.6, 48.1, 62.9, 70.7, 116.1, 126.7, 126.8, 127.4, 127.5, 127.6, 127.7, 127.8, 128.1, 128.9, 129.4, 132.7, 134.3, 138.0, 140.4, 145.9, 159.1, 163.5, 170.1, 172.9 ppm; Anal. Calcd. For  $C_{33}H_{31}ClN_2O_5$ : C, 69.41; H, 5.47; N, 4.91; Found: C, 69.28; H, 5.57; N, 4.75%

4.1.2.10. 2-Chloro-*N*-[(cyclohexylcarbamoyl)-(4-oxo-6-phenyl-4*H*-pyran-2-yl)-methyl]-*N*-phenylbenzamide (**12j**)

Yellow solid; Yield: 86%; mp: 57-59°C; FT-IR (KBr):  $\nu$  3292 (N-H), 3063 (aromatic C-H), 2927 (aliphatic C-H), 2854 (aliphatic C-H), 1694 (amide C=O), 1653 (pyrone C=O)  $\text{cm}^{-1}$ ;  $^1\text{H}$  NMR (400 MHz,  $\text{CDCl}_3$ ):  $\delta$  1.12–2.03 (m, 10H, 5 $\text{CH}_2$  of cyclohexyl), 3.90 (m, 1H, CH–N of cyclohexyl), 6.18 (s, 1H, C-H), 6.57 (s, 1H, pyrone-H), 6.62 (s, 1H, pyrone-H), 6.82 (bd, 1H,  $J=8$  Hz, N-H), 7.03-7.19 (m, 7H, Ar-H), 7.27-7.29 (m, 2H, Ar-H), 7.41-7.54 (m, 3H, Ar-H), 7.59 (d, 2H,  $J=8$ Hz, Ar-H) ppm;  $^{13}\text{C}$  NMR (100 MHz,  $\text{CDCl}_3$ ):  $\delta$  23.6, 23.7, 24.3, 31.6, 31.7, 48.2, 62.5, 109.8, 116.8, 124.7, 125.3, 127.6, 127.8, 127.9, 127.9, 128.3, 129.2, 129.3, 129.4, 130.5, 134.1, 137.9, 159.4, 162.5, 163.2, 167.9, 178.4 ppm; Anal. Calcd. For  $\text{C}_{32}\text{H}_{29}\text{ClN}_2\text{O}_4$ : C, 71.04; H, 5.40; N, 5.18; Found: C, 70.95; H, 5.43; N, 5.12%

4.1.2.11. *2-Chloro-N-[(cyclohexylcarbamoyl)-(4-oxo-6-phenyl-4H-pyran-2-yl)methyl]-N-p-tolylbenzamide (12k)*

Yellow solid; Yield: 89%; mp: 102-104°C; FT-IR (KBr):  $\nu$  3297 (N-H), 3064 (aromatic C-H), 2928 (aliphatic C-H), 2854 (aliphatic C-H), 1693 (amide C=O), 1653 (pyrone C=O)  $\text{cm}^{-1}$ ;  $^1\text{H}$  NMR (400 MHz,  $\text{CDCl}_3$ ):  $\delta$  1.18–2.03 (m, 10H, 5 $\text{CH}_2$  of cyclohexyl), 2.07 (s, 3H,  $\text{CH}_3$ ), 3.90 (m, 1H, CH–N of cyclohexyl), 6.17 (s, 1H, C-H), 6.59 (d, 1H,  $J=2$ Hz, pyrone-H), 6.65 (d, 1H,  $J=2$ Hz, pyrone-H), 6.78-6.83 (m, 3H, Ar-H, N-H), 7.06-7.19 (m, 6H, Ar-H), 7.41-7.51 (m, 3H, Ar-H), 7.59 (d, 2H,  $J=8$ Hz, Ar-H) ppm;  $^{13}\text{C}$  NMR (100 MHz,  $\text{CDCl}_3$ ):  $\delta$  19.9, 23.6, 23.7, 24.4, 31.7, 31.8, 48.2, 62.6, 109.9, 116.9, 124.8, 125.3, 127.5, 127.6, 127.9, 128.4, 128.5, 129.1, 129.2, 129.5, 130.6, 134.2, 135.3, 137.7, 159.5, 162.7, 163.3, 168.2, 178.6 ppm; Anal. Calcd. For  $\text{C}_{33}\text{H}_{31}\text{ClN}_2\text{O}_4$ : C, 71.41; H, 5.63; N, 5.05; Found: C, 71.25; H, 5.66; N, 5.01%

4.1.2.12. *N-[(tert-Butylcarbamoyl)-(4-oxo-6-phenyl-4H-pyran-2-yl)methyl]-N-p-tolylbenzamide (12l)*

Yellow solid; Yield: 82%; mp: 78-80°C; FT-IR (KBr):  $\nu$  3301 (N-H), 3062 (aromatic C-H), 2962 (aliphatic C-H), 2923 (aliphatic C-H), 2858 (aliphatic C-H), 1696 (amide C=O), 1650 (pyrone C=O)  $\text{cm}^{-1}$ ;  $^1\text{H}$  NMR (400 MHz,  $\text{CDCl}_3$ ):  $\delta$  1.39 (s, 9H, 3 $\text{CH}_3$ ), 2.14 (s, 3H,  $\text{CH}_3$ ), 6.00 (s, 1H, C-H), 6.56 (d, 1H,  $J=2$ Hz, pyrone-H), 6.63 (bs, 1H, N-H), 6.65 (d, 1H,  $J=2$ Hz, pyrone-H), 6.89 (d, 2H,  $J=8$ Hz, Ar-H), 7.05 (d, 2H,  $J=8$  Hz, Ar-H), 7.15-7.50 (m, 8H, Ar-H), 7.61 (d, 2H,  $J=8$ Hz, Ar-H) ppm;  $^{13}\text{C}$  NMR (100 MHz,  $\text{CDCl}_3$ ):  $\delta$  19.9, 27.5, 51.0, 64.9, 110.1, 116.0,

124.8, 126.8, 127.7, 127.9, 128.7, 129.2, 129.5, 129.7, 130.5, 133.7, 136.9, 137.3, 160.1, 162.6, 163.7, 170.3, 178.5 ppm; Anal. Calcd. For C<sub>31</sub>H<sub>30</sub>N<sub>2</sub>O<sub>4</sub>: C, 75.28; H, 6.11; N, 5.66; Found: C, 75.12; H, 6.17; N, 5.62%

4.1.2.13. *2-Chloro-N-[(cyclohexylcarbamoyl)-(4-oxo-6-phenyl-4H-pyran-2-yl)methyl]-N-(4-methoxyphenyl)benzamide (12m)*

Yellow solid; Yield: 76%; mp: 105-107°C; FT-IR (KBr):  $\nu$  3298 (N-H), 3065 (aromatic C-H), 2929 (aliphatic C-H), 2852 (aliphatic C-H), 1694 (amide C=O), 1653 (pyrone C=O) cm<sup>-1</sup>; <sup>1</sup>H NMR (400 MHz, CDCl<sub>3</sub>):  $\delta$  1.12–2.04 (m, 10H, 5CH<sub>2</sub> of cyclohexyl), 3.57 (s, 3H, CH<sub>3</sub>), 3.90 (m, 1H, CH–N of cyclohexyl), 6.21 (s, 1H, C-H), 6.51 (d, 2H, *J* = 8Hz, Ar-H), 6.59 (s, 1H, pyrone-H), 6.65 (s, 1H, pyrone-H), 6.74 (bd, 1H, *J* = 8Hz, N-H), 7.05-7.20 (m, 6H, Ar-H), 7.42-7.55 (m, 3H, Ar-H), 7.61 (d, 2H, *J* = 8Hz, Ar-H) ppm; <sup>13</sup>C NMR (100 MHz, CDCl<sub>3</sub>):  $\delta$  23.7, 23.8, 24.3, 31.6, 31.7, 48.2, 54.1, 62.2, 109.9, 112.9, 117.0, 124.7, 125.4, 127.4, 127.9, 128.3, 129.0, 129.1, 129.3, 130.2, 130.6, 130.8, 134.2, 158.1, 159.4, 162.6, 163.3, 168.4, 178.6 ppm; Anal. Calcd. For C<sub>33</sub>H<sub>31</sub>ClN<sub>2</sub>O<sub>5</sub>: C, 69.41; H, 5.47; N, 4.91; Found: C, 69.25; H, 5.51; N, 4.88 %

4.1.2.14. *N-[(tert-Butylcarbamoyl)-(4-oxo-6-phenyl-4H-pyran-2-yl)methyl]-2-chloro-N-(4-methoxyphenyl)benzamide (12n)*

Yellow solid; Yield: 74%; mp: 88-90°C; FT-IR (KBr):  $\nu$  3307 (N-H), 3066 (aromatic C-H), 2966 (aliphatic C-H), 2926 (aliphatic C-H), 2855 (aliphatic C-H), 1694 (amide C=O), 1653 (pyrone C=O) cm<sup>-1</sup>; <sup>1</sup>H NMR (400 MHz, CDCl<sub>3</sub>):  $\delta$  1.43 (s, 9H, 3CH<sub>3</sub>), 3.56 (s, 3H, CH<sub>3</sub>), 6.12 (s, 1H, C-H), 6.51 (d, 2H, *J* = 8Hz, Ar-H), 6.57 (d, 1H, *J* = 2Hz, pyrone-H), 6.64 (d, 1H, *J* = 2Hz, pyrone-H), 6.74 (bs, 1H, N-H), 7.04-7.19 (m, 6H, Ar-H), 7.42-7.50 (m, 3H, Ar-H), 7.63 (d, 2H, *J* = 8Hz, Ar-H) ppm; <sup>13</sup>C NMR (100 MHz, CDCl<sub>3</sub>):  $\delta$  27.5, 51.2, 54.1, 62.9, 109.9, 112.8, 116.9, 124.7, 125.3, 127.5, 127.9, 128.3, 129.0, 129.1, 129.5, 130.3, 130.5, 130.8, 134.3, 158.1, 159.5, 162.5, 163.4, 168.2, 178.5 ppm; Anal. Calcd. For C<sub>31</sub>H<sub>29</sub>ClN<sub>2</sub>O<sub>5</sub>: C, 68.31; H, 5.36; N, 5.14; Found: C, 68.14; H, 5.41; N, 5.10 %

4.2. MTT assay

RPMI 1640, fetal bovine serum (FBS), trypsin and phosphate buffered saline (PBS) were purchased from Biosera (Ringmer, UK). 3-(4, 5-Dimethylthiazol-2-yl)-2, 5-diphenyltetrazolium bromide (MTT) was obtained from Sigma-Aldrich (Saint Louis, MO, USA) and penicillin/streptomycin was purchased from Invitrogen (San Diego, CA, USA). Doxorubicin and dimethyl sulphoxide were obtained from EBEWE Pharma (Unterach, Austria) and Merck (Darmstadt, Germany), respectively. HL-60 (human promyelocytic leukemia), LS180 (human colon adenocarcinoma) and MCF-7 (human breast adenocarcinoma) cells were obtained from the National Cell Bank of Iran, Pasteur Institute, Tehran, Iran. Cell lines were maintained in RPMI 1640 supplemented with 100 units/ml penicillin-G and 100 µg/ml streptomycin as well as 10% FBS (except for HL-60 cells that needed 20% FBS). Cells were maintained at 37°C in humidified air containing 5% CO<sub>2</sub>. LS180 and MCF-7 cells were grown in monolayer cultures, while HL-60 cells were grown in suspension.

Cell viability following exposure to synthetic compounds was estimated by using the MTT reduction assay [38,42]. HL-60, LS180 and MCF-7 cells were plated in 96-well flat bottomed microplates at densities of 40,000, 50,000 and 30,000 cells/ml (100 µl per well), respectively. Control wells contained the same number of cells without any drugs, while blank wells contained only growth medium for background correction. After overnight incubation at 37 °C, half of the growth medium was removed and 50 µl of medium supplemented with 3-4 different concentrations of synthetic compounds were added in duplicate. Plates with HL-60 cells were centrifuged before this procedure. Compounds were all first dissolved in DMSO and then diluted in the growth medium. The maximum concentration of DMSO in the wells was 0.5%. Cells were further incubated for 72 hr and at the end of the incubation time fresh medium containing 0.5 mg/ml of MTT was added. Plates were incubated for another 4 hr at 37 °C. Then the formazan crystals formed inside viable cells were solubilized in 200 µl DMSO. The optical density was measured at 570 nm with background correction at 655 nm using a Bio-Rad microplate reader (Model 680). The percent inhibition of viability for each concentration of compound was calculated compared to the control wells and IC<sub>50</sub> values (concentration of the compound that induces 50% inhibition of cell viability) were calculated with the CurveExpert software version 1.34 for Windows. Each experiment was repeated 3-5 times. Data are presented as mean ± S.D.

### 4.3. QSAR analysis

#### 4.3.1. Descriptor generation

The chemical structure of molecules was constructed using HyperChem (Version 7, Hypercube Inc., <http://www.hyper.com>, USA). The Z-matrices of the structures were provided by the software and were then transferred to the Gaussian 98 program [43]. Complete geometry optimization was performed taking the most extended conformations as starting geometries. Semi-empirical molecular orbital calculations (AM1) of the structures were performed using Gaussian 98 program.

A large number of molecular descriptors were calculated using HyperChem (HyperCube Inc.), Gaussian 98 and Dragon (Todeschini, <http://www.disat.unimib.it/vhm/>) Packages. Gaussian 98 were employed for calculation of different quantum chemical descriptors including dipole moment (DM), local charges, HOMO and LUMO energies, hardness ( $\eta$ ); softness (S); electronegativity ( $\chi$ ); and electrophilicity ( $\omega$ ). Dragon software was used to calculate different descriptors including functional groups, topological, geometrical, constitutional, charge descriptors and aromaticity indices for each molecule. Some chemical parameters including molecular volume (MV), molecular surface area (SA), hydrophobicity (logP) and hydration energy (HE) were calculated using HyperChem software.

#### 4.3.2. Data processing and modeling

The calculated descriptors were collected in a data matrix, **D**. First the descriptors were checked for constant or near constant values and those detected were removed from the original data matrix. Then, the correlation of descriptors with each other and with the activity data was determined. Among the collinear descriptors detected ( $r > 0.9$ ), one of them that had the highest correlation with activity was retained and the rest were omitted. MLR analysis with stepwise selection and elimination of variables was applied for developing QSAR models using SPSS software (SPSS Inc., version 17). The resulted models were validated by leave-one out cross-validation procedure (using MATLAB software) to check their predictive ability and robustness.

### 4.4. Molecular docking study

The docking studies were carried out using AutoDock 4.2 (The Scripps Research Institute, La Jolla, CA, <http://autodock.scripps.edu/>). Lamarckian Genetic Algorithm of the AutoDock 4.2 program was used to perform the flexible-ligand docking studies (Morris et al. 2009). Receptor X-ray crystal structure in complex with the inhibitor, 1-[4-[4-amino-5-(3-methoxyphenyl)-7H-pyrrolo[2,3- D]pyrimidin-7-yl]benzyl]piperidin-4-ol (S03) (PDB ID 1YOL; <http://www.pdb.org/>) [39] was obtained from the Brookhaven protein data bank. All pre-processing procedures of target protein and ligand files were performed within Accelrys ViewerLite 5.0 software and AutoDock Tools 1.5.4 program (ADT) which has been released as an extension suite to the Python Molecular Viewer [44]. The three-dimensional structures of the ligands were constructed using Chem3D Ultra 8.0 software [Chemical Structure Drawing Standard; Cambridge Soft Corporation, USA (2003)] to obtain standard 3D structures (pdb format). The constructed compounds were energetically minimized (100 steepest descent steps using MM<sup>+</sup> force field with a gradient convergence value of 0.1 kcal/mol ) using HyperChem (HyperCube Inc.).

For docked ligands, non-polar hydrogens were added; Gasteiger charges and torsions degrees of freedom were also allocated by ADT program. One-hundred independent genetic algorithm (GA) runs were considered for each ligand under study. For Lamarckian GA method, a maximum number of 2,500,000 energy evaluations; 27,000 maximum generations; a gene mutation rate of 0.02; and a crossover rate of 0.8 were used. A grid of 40×40× 40 points in x, y, and z direction with grid spacing of 0.375 Å<sup>o</sup> was built centered on the center of mass of the catalytic site. Cluster analysis was performed on the docked results using a root mean square (RMS) tolerance of 2 Å<sup>o</sup>. Ranking of the clusters was carried out according to the obtained average lowest binding energy of members of the cluster to highest.

### **Acknowledgments**

The authors wish to thank the Research Council of University of Tabriz and Shiraz University of Medical Sciences for their financial support.

## References

- [1] F. Caturla, M. Amat, R.F. Reinoso, M. Cordoba, G. Warreallow, Racemic and chiral sulfoxides as potential prodrugs of the COX-2 inhibitors Vioxx and Arcoxia, *Bioorg. Med. Chem. Lett.* 16 (2006) 3209-3212.
- [2] P.W. Groundwater, K.R.H. Solomons, The synthesis of pyranoacridinone inhibitors of protein tyrosine kinases, *J. Chem. Soc. Perkin Trans. 1* (1994) 173-177.
- [3] T. Kamino, K. Kuramochi, S. Kobayashi, A concise approach to 5-substituted-pyrones from kojic acid, *Tetrahedron Lett.* 44 (2003) 7349-7351.
- [4] D.T. Puerta, J. Mongan, B.L. Tran, J.A. McCammon, S.M. Cohen, Potent, selective pyrone-based inhibitors of stromelysin-1, *J. Am. Chem. Soc.* 127 (2005) 14148-14149.
- [5] Y.L. Yan, S.M. Cohen, Efficient synthesis of 5-amido-3-hydroxy-4-pyrones as inhibitors of matrix metalloproteinases, *Org. Lett.* 9 (2007) 2517-2520.
- [6] G. Ding, L. Jiang, L. Guo, X. Chen, H. Zhang, Y. Che, Pestalazines and pestalamides, bioactive metabolites from the plant pathogenic fungus *Pestalotiopsis theae*, *J. Nat. Prod.* 71 (2008) 1861-1865.
- [7] J.C. Henrikson, T.K. Ellis, J.B. King, R.H. Cichewicz, Reappraising the structures and distribution of metabolites from black aspergilli containing uncommon 2-benzyl-4*H*-pyran-4-one and 2-benzylpyridin-4(1*H*)-one systems, *J. Nat. Prod.* 74 (2011) 1959-1964.
- [8] D.H. Li, S.X. Cai, L. Tian, Z.J. Lin, T.J. Zhu, Y.C. Fang, P.P. Liu, Q.Q. Gu, W.M. Zhu, Two new metabolites with cytotoxicities from deep-sea fungus, *Aspergillus sydowi* YH11-2, *Arch. Pharmacol. Res.* 30 (2007) 1051-1054.
- [9] R.C. Barcelos, J.C. Pastre, V. Caixeta, D.B. Vendramini-Costa, J.E. de Carvalho, R.A. Pilli, Synthesis of methoxylated goniothalamins, aza-goniothalamins and gamma-pyrones and their *in vitro* evaluation against human cancer cells, *Bioorg. Med. Chem.* 20 (2012) 3635-3651.
- [10] J. Bransova, M. Uher, L. Novotny, J. Brtko, 5-benzoyloxy-2-thiocyanatomethyl-4-pyrone, a novel heterocyclic compound: synthesis, structure determination and effects on neoplastic cell growth, *Anticancer Res.* 17 (1997) 1175-1178.
- [11] J. Brtko, L. Rondahl, M. Fickova, D. Hudecova, V. Eybl, M. Uher, Kojic acid and its derivatives: history and present state of art, *Cent. Eur. J. Public Health.* 12 Suppl (2004) S16-18.

- [12] J. Farard, G. Lanceart, C. Loge, M.R. Nourrisson, F. Cruzalegui, B. Pfeiffer, M. Duflos, Design, synthesis and evaluation of new 6-substituted-5-benzyloxy-4-oxo-4*H*-pyran-2-carboxamides as potential Src inhibitors, *J. Enzym. Inhib. Med. Chem.* 23 (2008) 629-640.
- [13] M. Susva, M. Missbach, J. Green, Src inhibitors: drugs for the treatment of osteoporosis, cancer or both?, *Trends Pharmacol. Sci.* 21 (2000) 489-495.
- [14] J.M. Summy, G.E. Gallick, Src family kinases in tumor progression and metastasis, *Cancer Metastasis Rev.* 22 (2003) 337-358.
- [15] A.P. Belsches-Jablonski, M.L. Demory, J.T. Parsons, S.J. Parsons, The Src pathway as atherapeutic strategy, *Drug. Discov. Today Ther. Strat.* 2 (2005) 313-321.
- [16] I. Ugi, A. Domling, B. Werner, Since 1995 the new chemistry of multicomponent reactions and their libraries, including their heterocyclic chemistry, *J. Heterocyclic Chem.* 37 (2000) 647-658.
- [17] A. Domling, I. Ugi, Multicomponent reactions with isocyanides, *Angew. Chem. Int. Ed. Engl.* 39 (2000) 3168-3210.
- [18] M. Passerini, L. Simone, Sopra gli isonitrili (I). Composto del p-isonitrilazobenzolo con Acetone ed acido acetico, *Gazz. Chim. Ital.* 52 (1921) 126-129.
- [19] C.C. Musonda, D. Taylor, J. Lehman, J. Gut, P.J. Rosenthal, K. Chibale, Application of multi-component reactions to antimalarial drug discovery. Part 1: Parallel synthesis and antiplasmodial activity of new 4-aminoquinoline Ugi adducts, *Bioorg. Med. Chem. Lett.* 14 (2004) 3901-3905.
- [20] C.M. Haney, C. Schneider, B. Beck, J.L. Brodsky, A. Domling, Identification of Hsp70 modulators through modeling of the substrate binding domain, *Bioorg. Med. Chem. Lett.* 19 (2009) 3828-3831.
- [21] P.G. Wyatt, M.J. Allen, A.D. Borthwick, D.E. Davies, A.M. Exall, R.J. Hatley, W.R. Irving, D.G. Livermore, N.D. Miller, F. Nerozzi, S.L. Sollis, A.K. Szardenings, 2,5-Diketopiperazines as potent and selective oxytocin antagonists 1: Identification, stereochemistry and initial SAR, *Bioorg. Med. Chem. Lett.* 15 (2005) 2579-2582.
- [22] H.J. Sanganee, A. Baxter, S. Barber, A.J. Brown, D. Grice, F. Hunt, S. King, D. Laughton, G. Pairaudeau, B. Thong, R. Weaver, J. Unitt, Discovery of small molecule human C5a receptor antagonists, *Bioorg. Med. Chem. Lett.* 19 (2009) 1143-1147.

- [23] I.W. Ku, S. Cho, M.R. Doddareddy, M.S. Jang, G. Keum, J.H. Lee, B.Y. Chung, Y. Kim, H. Rhim, S.B. Kang, Morpholin-2-one derivatives as novel selective T-type  $\text{Ca}^{2+}$  channel blockers, *Bioorg. Med. Chem. Lett.* 16 (2006) 5244-5248.
- [24] D.J. Parks, L.V. Lafrance, R.R. Calvo, K.L. Milkiewicz, V. Gupta, J. Lattanze, K. Ramachandren, T.E. Carver, E.C. Petrella, M.D. Cummings, D. Maguire, B.L. Grasberger, T. Lu, 1,4-Benzodiazepine-2,5-diones as small molecule antagonists of the HDM2-p53 interaction: discovery and SAR, *Bioorg. Med. Chem. Lett.* 15 (2005) 765-770.
- [25] K. Groebke Zbinden, D.W. Banner, J. Ackermann, A. D'Arcy, D. Kirchhofer, Y.H. Ji, T.B. Tschopp, S. Wallbaum, L. Weber, Design of selective phenylglycine amide tissue factor/factor VIIa inhibitors, *Bioorg. Med. Chem. Lett.* 15 (2005) 817-822.
- [26] N.A. Yehia, W. Antuch, B. Beck, S. Hess, V. Schauer-Vukasinovic, M. Almstetter, P. Furer, E. Herdtweck, A. Domling, Novel nonpeptidic inhibitors of HIV-1 protease obtained via a new multicomponent chemistry strategy, *Bioorg. Med. Chem. Lett.* 14 (2004) 3121-3125.
- [27] X. Fan, X. Zhang, C. Bories, P.M. Loiseau, P.F. Torrence, The Ugi reaction in the generation of new nucleosides as potential antiviral and antileishmanial agents, *Bioorg. Chem.* 35 (2007) 121-136.
- [28] A. Arabanian, M. Mohammadnejad, S. Balalaie, J.H. Gross, Synthesis of novel Gn-RH analogues using Ugi-4MCR, *Bioorg. Med. Chem. Lett.* 19 (2009) 887-890.
- [29] A. Shahrissa, M. Saraei, Synthesis of pyrone carbaldehydes, pyrone sulfonium ylides and related epoxides, *J. Heterocyclic Chem.* 46 (2009) 268-272.
- [30] A. Shahrissa, R. Miri, S. Esmati, M. Saraei, A.R. Mehdipour, M. Sharifi, Synthesis and calcium channel antagonist activity of novel 1,4-dihydropyridine derivatives possessing 4-pyrone moieties, *Med. Chem. Res.* 21 (2012) 284-292.
- [31] A. Shahrissa, Z. Ghasemi, Synthesis of fused pyrimidone derivatives of 4-pyrones from the acetates of Baylis–Hillman adducts, *Chem. Heterocyclic Compd.* 46 (2010) 30-36.
- [32] A. Shahrissa, Z. Ghasemi, M. Saraei, Synthesis of 2,6-bis(1*H*-indole-6-yl)-4*H*-pyran-4-ones via Leimgruber–Batcho indole synthesis, *J. Heterocyclic Chem.* 46 (2009) 273-277.
- [33] A.F. Thomas, A. Marxer, Heilmittelchemische Studien in der heterocyclischen Reihe. 30. Mitteilung. Die Reaktion von Kojis ure mit Hydrazin. 2. Teil. Umsetzung von Kojis ure them mit Hydrazin, *Helv. Chim. Acta.* 43 (1960) 469-477.

- [34] M. Rudas, I. Fejes, M. Nyerges, A. Szöllösy, L. Tőke, P.W. Groundwater, Substituent effects on the  $4\pi + 2\pi$  cycloadditions of 4*H*-pyran-4-one derivatives J. Chem. Soc., Perkin Trans. 1 (1999) 1167-1172.
- [35] D. Hobuss, S. Laschat, A. Baro, Concise two-step synthesis of  $\gamma$ -pyrone from acetone, *synlett* (2005) 123-124.
- [36] V.I. Tyvorskii, D.N. Bobrov, O.G. Kulinkovich, N. De Kimpe, K.A. Tehrani, New synthetic approaches to 2-perfluoroalkyl-4*H*-pyran-4-ones, *Tetrahedron*, 54 (1998) 2819-2826.
- [37] H. Arimoto, S. Nishiyama, S. Yamamum, Mild conditions for cyclization of  $\beta$ -triketides to the corresponding  $\gamma$ -pyrones carrying adjacent chiral center toward biomimetic synthesis of fully substituted  $\gamma$ -pyrone-containing natural products, *Tetrahedron Lett.* 31 (1990) 5619-5620.
- [38] T. Mosmann, Rapid colorimetric assay for cellular growth and survival: application to proliferation and cytotoxicity assays, *J. Immunol. Methods* 65 (1983) 55-63.
- [39] C.B. Breitenlechner, N.A. Kairies, K. Honold, S. Scheiblich, H. Koll, E. Greiter, S. Koch, W. Schafer, R. Huber, R.A. Engh, Crystal structures of active SRC kinase domain complexes, *J. Mol. Biol.* 353 (2005) 222-231.
- [40] Y. Fukunishi, Y. Mikami, H. Nakamura, Similarities among receptor pockets and among compounds: analysis and application to in silico ligand screening, *J. Mol. Graph. Model.* 24 (2005) 34-45.
- [41] J. Pan, G.Y. Liu, J. Cheng, X.J. Chen, X.L. Ju, CoMFA and molecular docking studies of benzoxazoles and benzothiazoles as CYP450 1A1 inhibitors, *Eur. J. Med. Chem.* 45 (2010) 967-972.
- [42] R. Miri, O. Firuzi, P. Peymani, M. Zamani, A.R. Mehdipour, Z. Heydari, M.M. Farahani, A. Shafiee, Synthesis, cytotoxicity, and QSAR study of new aza-cyclopenta[b]fluorene-1,9-dione derivatives, *Chem. Biol. Drug Des.* 79 (2012) 68-75.
- [43] M.J. Frisch, G.W. Trucks, H.B. Schlegel, G.E. Scuseria, M.A. Robb, J.R. Cheeseman, V.G. Zakrzewski, J.A. Montgomery Jr., R.E. Stratmann, J.C. Burant, S. Dapprich, J.M. Millam, A.D. Daniels, K.N. Kudin, M.C. Strain, Ö. Farkas, J. Tomasi, V. Barone, M. Cossi, R. Cammi, B. Mennucci, C. Pomelli, C. Adamo, S. Clifford, J. Ochterski, G.A. Petersson, P.Y. Ayala, Q. Cui, K. Morokuma, P. Salvador, J.J. Dannenberg, D.K. Malick, A.D. Rabuck, K. Raghavachari, J.B. Foresman, J. Cioslowski, J.V. Ortiz, A.G. Baboul, B.B. Stefanov, G. Liu, A. Liashenko, P.

Piskorz, I. Komáromi, R. Gomperts, R.L. Martin, D.J. Fox, T. Keith, M.A. Al-Laham, C.Y. Peng, A. Nanayakkara, M. Challacombe, P.M.W. Gill, B. Johnson, W. Chen, M.W. Wong, J.L. Andres, C. Gonzalez, M. Head-Gordon, E.S. Replogle, J.A. Pople, *Gaussian 98* (Gaussian, Inc., Pittsburgh, PA, 1998).

[44] G.M. Morris, R. Huey, W. Lindstrom, M.F. Sanner, R.K. Belew, D.S. Goodsell, A.J. Olson, AutoDock4 and AutoDockTools4: Automated docking with selective receptor flexibility, *J. Comput. Chem.* 30 (2009) 2785-2791.

**Captions:**

**Fig. 1.** Chemical structure of some of biologically active pyrones.

**Fig. 2.** Substitution pattern of bis-carboxamide derivatives of 4-pyrone

**Fig. 3.** Plot of the predicted activity against the experimental activity for the QSAR model obtained by Equation 1 in HL-60 cell line.

**Fig. 4.** Best docked pose of compound **12n** (A) and **12k** (B) docked into Src tyrosine kinase ATP-binding site.

**Scheme 1.** Mechanism of the Ugi reaction.

**Scheme 2.** Synthesis of 4-pyrone carbaldehyde derivatives. Reagents and conditions: i) PhCH<sub>2</sub>Br (1 eq), NaOH (1eq), MeOH/H<sub>2</sub>O: 10/1, 60°C, 4h, 75%; ii) MnO<sub>2</sub> (8eq), CH<sub>2</sub>Cl<sub>2</sub>, rt., 3days, 65%; iii) (2eq), DME, reflux, 4h, 67%; iv) H<sub>2</sub>SO<sub>4</sub>, rt., 4h, 62%; v) NaBH<sub>4</sub> (4eq), MeOH, reflux, 3h, 42%; vi) MnO<sub>2</sub> (8eq), CH<sub>2</sub>Cl<sub>2</sub>, rt., 3days, 62%.

**Scheme 3.** General description of Ugi adducts.

**Table 1.** Chemical structures of bis-carboxamide derivatives of 4-pyrones **12a-n**.

**Table 2.** Cytotoxic activity of bis-carboxamide derivatives of pyrone **12a-n**.

**Table 3.** Statistical equations obtained by QSAR analysis.

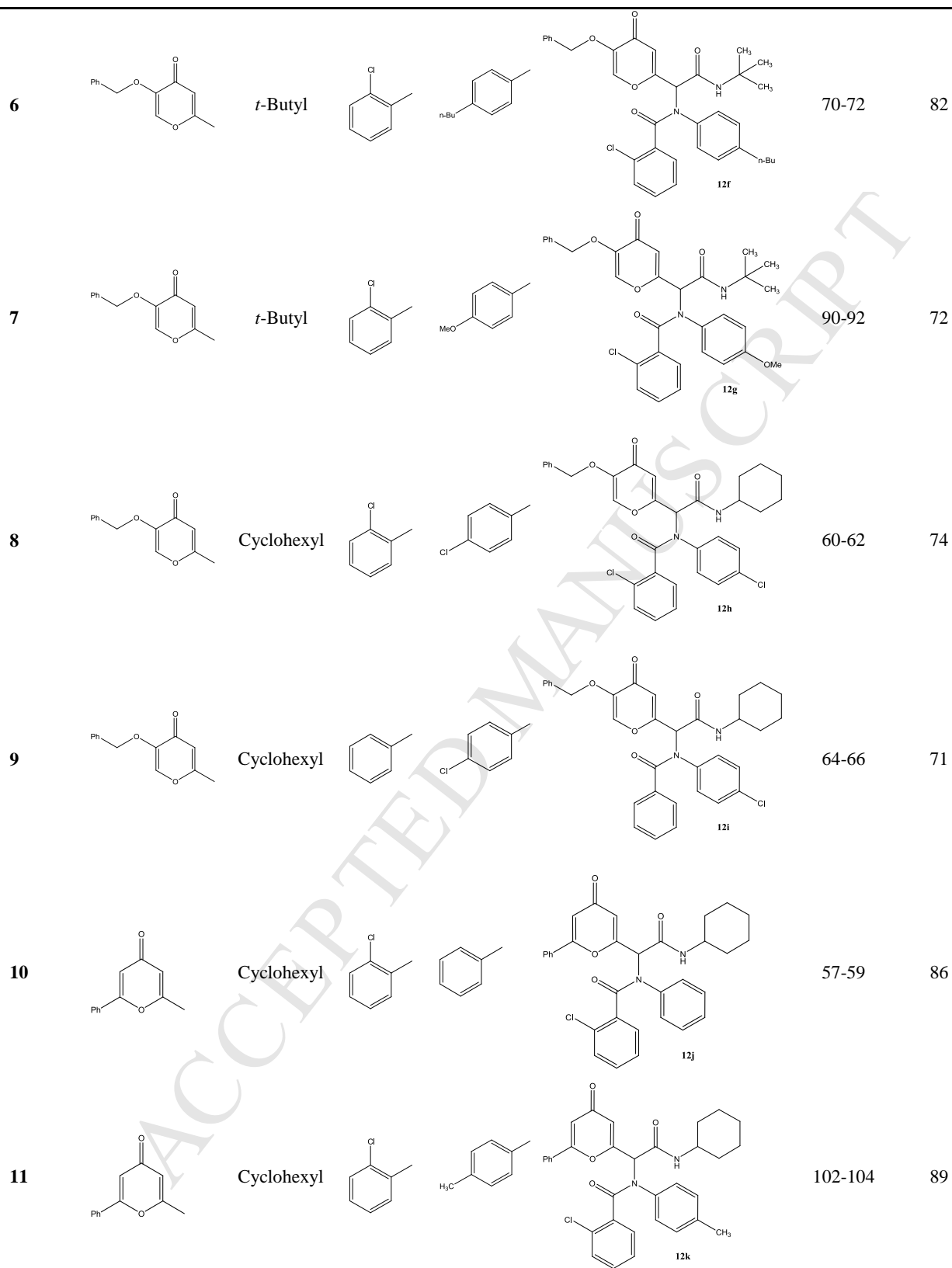
**Table 4.** Data of the selected descriptors used in this study and the experimental and predicted values of pIC<sub>50</sub> in HL-60 cell line.

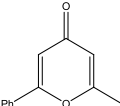
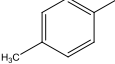
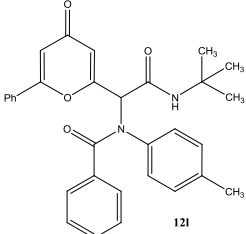
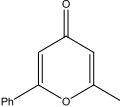
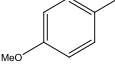
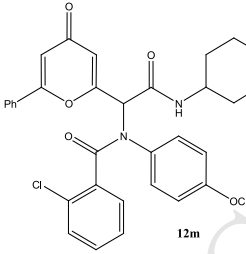
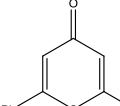
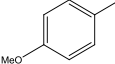
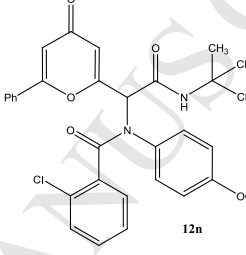
**Table 5.** The results of docking validation study obtained by re-docking of cognate ligand "1-{4-[4-amino-5-(3-methoxyphenyl)-7H-pyrrolo[2,3-D]pyrimidin-7-yl]benzyl}piperidin-4-ol (S03)" into Src tyrosine kinase.

**Table 6.** Results of docking study of synthesized bis-amide derivatives of 4-pyrones docked into Src tyrosine kinase active site.

**Table 1.** Chemical structures of bis-carboxamide derivatives of 4-pyrones **12a-n**

Entry	R <sub>1</sub>	R <sub>2</sub>	R <sub>3</sub>	R <sub>4</sub>	Product	m.p. (°C)	Yield (%)
1		Cyclohexyl				65-67	84
2		<i>t</i> -Butyl				62-63	78
3		Cyclohexyl				67-68	88
4		<i>t</i> -Butyl				60-62	85
5		Cyclohexyl				95-97	78



12		<i>t</i> -Butyl				78-80	82
13		Cyclohexyl				105-107	76
14		<i>t</i> -Butyl				88-90	74

**Table 2.** Cytotoxic activity of bis-carboxamide derivatives of pyrone **12a-n**.

Compound	IC <sub>50</sub> (μM)		
	LS180 cells	MCF-7 cells	HL-60 cells
12a	97.3(±5.1)	84.2(±14.6)	66.2(±4.5)
12b	Inactive	63.1(±9.6)	57.3(±0.5)
12c	63.0(±7.2)	56.3(±11.6)	12.1(±0.9)
12d	88.3(±5.9)	53.8(±8.9)	42.0(±3.6)
12e	20.2(±2.0)	11.2(±2.1)	11.3(±1.9)
12f	88.2(±13.3)	28.6(±4.2)	16.2(±2.1)
12g	77.3(±7.5)	47.2(±6.6)	52.9(±4.2)
12h	Inactive	168.5(±24.1)	30.5(±5.2)
12i	Inactive	Inactive	14.7(±0.9)
12j	Inactive	Inactive	72.0(±8.8)
12k	Inactive	Inactive	22.2(±4.9)
12l	121.8(±18.0)	54.9(±7.1)	33.0(±1.8)
12m	Inactive	Inactive	Inactive

12n	16.1( $\pm$ 1.2)	9.1( $\pm$ 0.9)	13.8( $\pm$ 5.2)
Cisplatin	10.0( $\pm$ 1.7)	26.2( $\pm$ 8.4)	3.2( $\pm$ 0.8)
Doxorubicin	0.04( $\pm$ 4.7)	0.2 ( $\pm$ 22.1)	0.01( $\pm$ 1.8)

Values in parentheses represent the average of 3-4 experiments  $\pm$  S.E.M.

**Table 3.** Statistical equations obtained by QSAR analysis.

Cell line	Equation	R <sup>2</sup>	S.E <sup>a</sup>	Q <sup>2</sup>	RMScv	n <sup>b</sup>
HL-60	E1: Y= -1.35( $\pm$ 0.16) HGM -15.24 ( $\pm$ 3.2) ISH + 1.34( $\pm$ 0.40) PJI <sub>2</sub> +23.0 ( $\pm$ 3.05)	0.93	0.09	0.83	0.13	13

<sup>a</sup> Standard error of regression

<sup>b</sup> Number of compounds used for QSAR analysis

**Table 4.** Data of the selected descriptors used in this study and the experimental and predicted values of pIC<sub>50</sub> in HL-60 cell line.

Compound	Descriptors			pIC <sub>50</sub>	
	HGM	ISH	PJI <sub>2</sub>	Experimental	Predicted
12a	3.59	1.00	1.00	4.18	4.31
12b	3.60	1.00	1.00	4.24	4.27
12c	3.40	0.98	1.00	4.92	4.75
12d	3.48	1.00	1.00	4.38	4.43
12e	3.14	0.99	1.00	4.95	5.06
12f	3.10	1.00	0.90	4.79	4.82
12g	3.52	0.99	0.89	4.28	4.37
12h	3.51	0.99	1.00	4.52	4.51
12i	3.31	0.99	1.00	4.83	4.78
12j	3.61	1.00	0.86	4.14	3.99
12k	3.40	0.97	0.86	4.65	4.94
12l	3.47	0.99	0.86	4.48	4.37
12n	3.33	0.99	1.00	4.86	4.76

**Table 5.** The results of docking validation study obtained by re-docking of cognate ligand "1-{4-[4-amino-5-(3-methoxyphenyl)-7H-pyrrolo[2,3-D]pyrimidin-7-yl]benzyl}piperidin-4-ol (S03)" into Src tyrosine kinase.

Binding pose of S03 into Srs tyrosine kinase ATP binding site	$\Delta G_b^a$ (kcal/mol)	$K_i^b$ (nM)	RMSD from reference ( $\text{Å}^\circ$ )
	-9.07	0.223	1.463

<sup>a</sup> binding free energy

<sup>b</sup> Inhibition constant

**Table 6.** Results of docking study of synthesized bis-amide derivatives of 4-pyrones docked into Src tyrosine kinase active site.

compound	$\Delta G_b$ (kcal/mol)	$K_i$ ( $\mu\text{M}$ )	Hydrogen bond between atom of compounds and aminoacids of Src-kinase active site		
			Atom of ligand*	Amino acid	Distance ( $\text{Å}^\circ$ )
12a	-9.48	0.113	(4-Pyrone) C=O	Met 343	3.07
12b	-7.32	4.28	(benzoyl)C=O,	Leu275	2.47,
			( <i>t</i> -Butyl carboxamide) C=O	Leu275	2.99
			( <i>t</i> -Butyl amide) NH	Asp350	2.05

12c	-8.25	0.904	(Cyclohexyl carboxamide) <b>NH</b>	Leu275	1.97
			(2-Chlorobenzoyl) <b>C=O</b>	Ser347	3.08
12d	-7.65	2.47	( <i>t</i> -Butyl carboxamide) <b>NH</b>	Leu275	1.82
			(2-Chlorobenzoyl) <b>C=O</b>	Ser347	3.13
12e	-8.36	0.742	(4-Pyrone) <b>C=O</b>	Met 343-	3.35
12f	-7.16	5.66	( <i>t</i> -Butyl carboxamide) <b>NH</b>	Leu275	2.09
			(4-Pyrone) <b>C=O</b>	Gln277	2.92
			( <i>t</i> -Butyl carboxamide) <b>C=O</b>	Asp350	2.67
12g	-8.32	0.801	(4-Pyrone) <b>C=O</b>	Leu275	2.29
			( <i>t</i> -Butyl carboxamide) <b>NH</b>	Met343	3.26
12h	-8.62	0.483	-	-	-
12i	-8.20	0.977	-	-	-
12j	-9.35	0.141	(4-Pyrone) <b>C=O</b>	Met343	2.65
12k	-9.74	0.0724	(Cyclohexyl carboxamide) <b>NH</b>	Leu275	2.44
			(4-Pyrone) <b>C=O</b>	Met343	2.70, 2.69
12l	-8.79	0.360	(benzoyl) <b>C=O</b>	Ser347	2.97
			(4-Pyrone) <b>C=O</b>	Ala392, Asp406	2.76, 2.75
12m	-8.33	0.789	(4-Pyrone) <b>C=O</b>	Asp 350	3.09
12n	-9.87	0.0582	(Methyl ether) <b>CH<sub>3</sub>O</b>	Met343	2.93
			(4-Pyrone) <b>C=O</b>	Ala392, Asp406	2.74, 2.83

\*The ligand's atom participating in H-bond interaction is demonstrated as bold style.

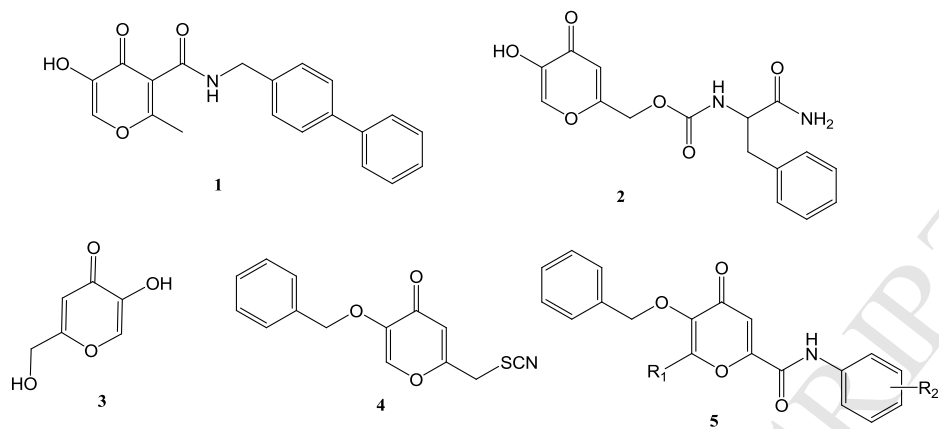


**Fig. 1.** Chemical structure of some of biologically active pyrones.

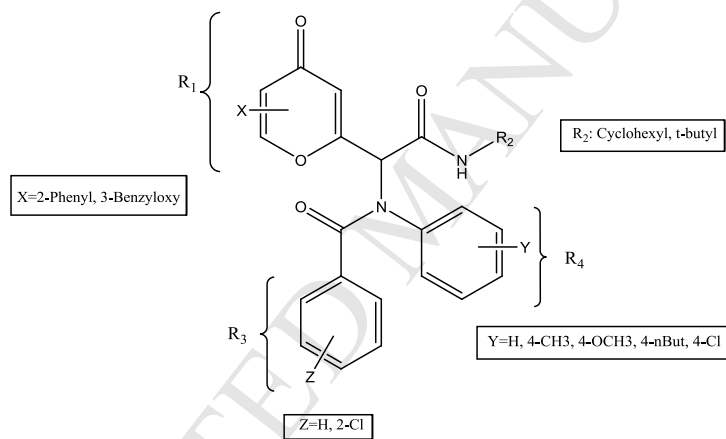


**Fig. 2.** Substitution pattern of bis-carboxamide derivatives of 4-pyrene

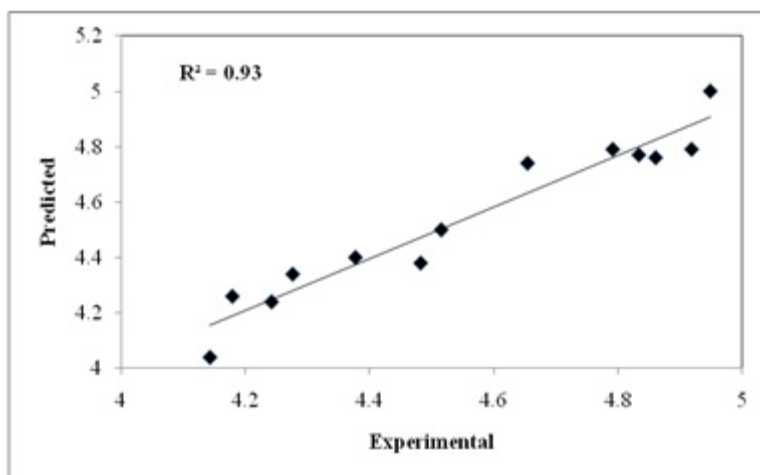


**Fig. 3.** Plot of the predicted activity against the experimental activity for the QSAR model obtained by Equation 1 in HL-60 cell line.

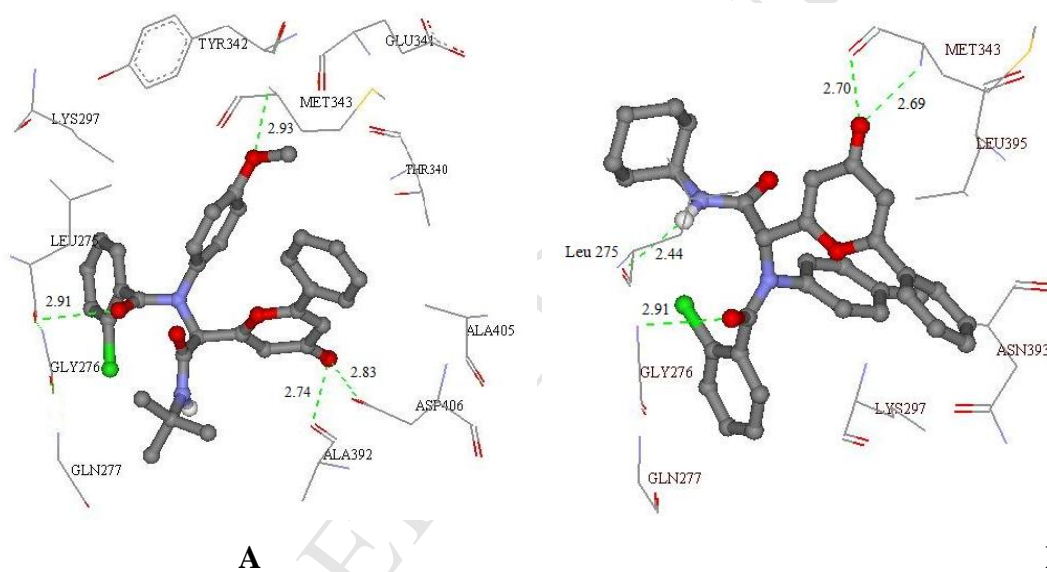
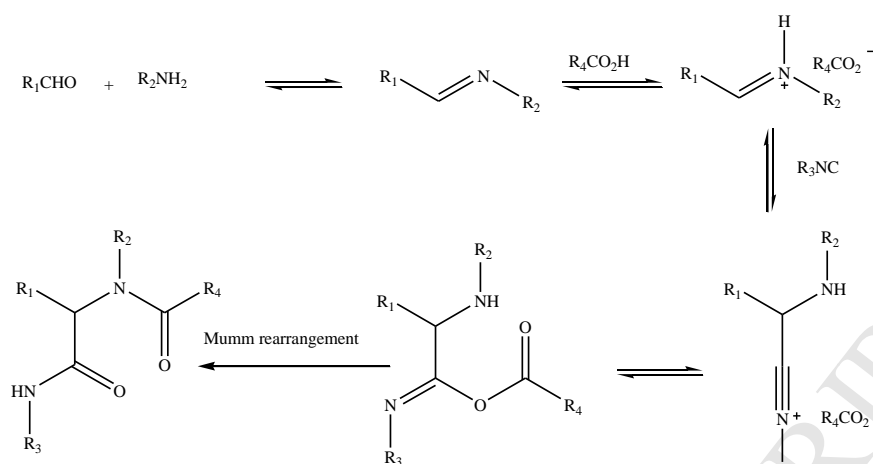
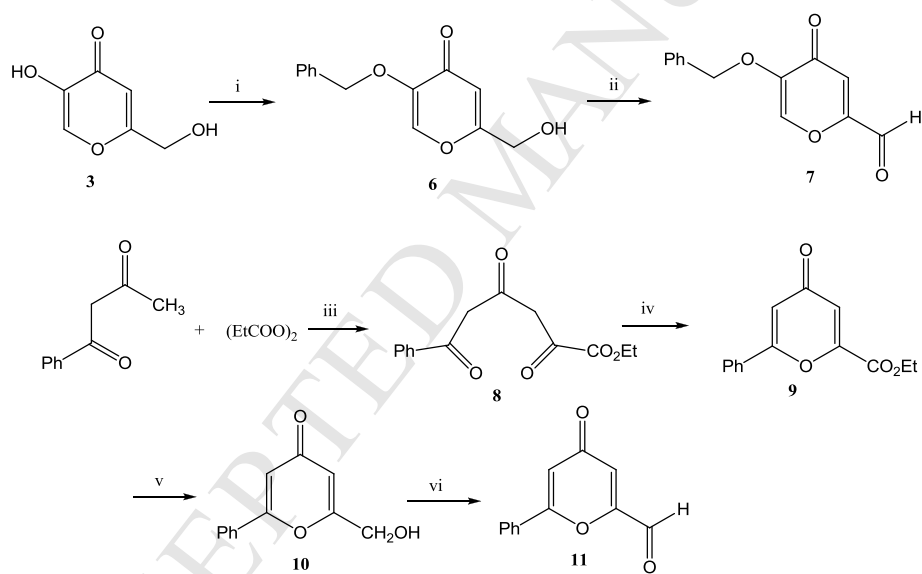


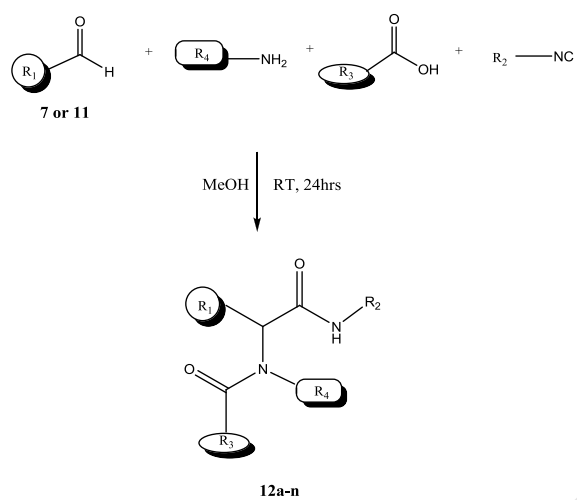
**Fig. 4.** Best docked pose of compound **12n** (A) and **12k** (B) docked into Src tyrosine kinase ATP-binding site.



**Scheme 1.** Mechanism of the Ugi reaction



**Scheme 2.** Synthesis of 4-pyrone carbaldehyde derivatives. Reagents and conditions: i) PhCH<sub>2</sub>Br (1 eq), NaOH (1eq), MeOH/H<sub>2</sub>O: 10/1, 60°C, 4h, 75%; ii) MnO<sub>2</sub> (8eq), CH<sub>2</sub>Cl<sub>2</sub>, rt., 3days, 65%; iii) (2eq), DME, reflux, 4h, 67%; iv)H<sub>2</sub>SO<sub>4</sub>, rt., 4h, 62%; v) NaBH<sub>4</sub> (4eq), MeOH, reflux, 3h, 42%; vi) MnO<sub>2</sub> (8eq), CH<sub>2</sub>Cl<sub>2</sub>, rt., 3days, 62%.



**Scheme 3.** General description of Ugi adducts